



HAL
open science

Use of Electrical Resistivity Tomography measurements for investigation of different grouting materials for very shallow geothermal applications within varying seasonal conditions; applied on a geothermal Earth-Air Heat Exchanger system.

Hans Schwartz, Jian Lin, David Bertermann

► To cite this version:

Hans Schwartz, Jian Lin, David Bertermann. Use of Electrical Resistivity Tomography measurements for investigation of different grouting materials for very shallow geothermal applications within varying seasonal conditions; applied on a geothermal Earth-Air Heat Exchanger system.. *Renewable Energy*, 2024, 228, 10.1016/j.renene.2024.120664 . hal-04589924v2

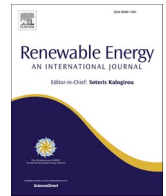
HAL Id: hal-04589924

<https://hal.science/hal-04589924v2>

Submitted on 5 Jul 2024

HAL is a multi-disciplinary open access archive for the deposit and dissemination of scientific research documents, whether they are published or not. The documents may come from teaching and research institutions in France or abroad, or from public or private research centers.

L'archive ouverte pluridisciplinaire **HAL**, est destinée au dépôt et à la diffusion de documents scientifiques de niveau recherche, publiés ou non, émanant des établissements d'enseignement et de recherche français ou étrangers, des laboratoires publics ou privés.



Use of electrical resistivity tomography measurements for investigation of different grouting materials for very shallow geothermal applications within varying seasonal conditions; Applied on a geothermal earth-air heat exchanger system

Hans Schwarz^{a,*}, Jian Lin^b, David Bertermann^a

^a GeoZentrum Nordbayern, Department Geographie und Geowissenschaften, Friedrich-Alexander-Universität Erlangen-Nürnberg, Schlossgarten 5, 91054, Erlangen, Germany

^b ICUBE(UMR7357), IUT Robert Schuman, University of Strasbourg, 67400, Illkirch-Graffenstaden, France

ARTICLE INFO

Keywords:

Electrical resistivity tomography
Soil properties
Earth air-heat exchanger
Very shallow geothermal
Grouting material
Seasonal impact

ABSTRACT

To achieve the current climate targets, heat pump systems like very shallow geothermal applications are gaining ground. However, the dimensioning of these ground coupled systems is soil-dependent and thus subject to significant differences in efficiency. Furthermore, the thermal properties of the grouting materials are essential for heat transfer in the direct vicinity of the geothermal application. To provide a non-invasive assessment of relevant soil and grouting characteristics, electrical resistivity tomography (ERT) measurements were performed.

In this case, the surrounding of an Earth Air-Heat Exchanger – system (EAHE) with different grouting materials (fine sand and fine sand with bentonite) was investigated. For investigation the electrical resistivity (ER) of initial and modified soil conditions were measured regarding soil texture and moisture content. Thereby, the different grouting materials are clearly identified. Thus, based on the ERT measurements, a characterisation of key soil and grouting material properties for applications focusing on heat transfer in soil has been carried out.

Furthermore, the depth of soil disturbance due to the EAHE installation could have been traced.

Due to a monitoring over different season (February and May) changes in raw ER data could have been ascribed to temperature changes.

1. Introduction

Renewable energies are indispensable for meeting climate targets and for increasing independence from the import of fossil fuels. For meeting the demand of thermal and cooling energy, very shallow geothermal systems can play an important role.

One general difficulty of very shallow geothermal systems is the determination of an accurate dimension to meet particular energy demands. For installations of vertical borehole heat exchangers Thermal Response Tests (TRT) can be performed [1–3] even though neighbourhood effects may occur [4,5], but for horizontal very shallow systems such a standardised process is not yet established. This is also due to a bright variety of very shallow geothermal systems [6] and due to the easy adaptability of the systems configuration, which also shows a performance influence [7]. Regarding very shallow geothermal

applications, to make economies usually an appropriate soil assessment for a proper and soil depending installation is not commissioned. In addition, the grouting material in the immediate vicinity of the ground source heat exchanger (GSHE) also has a major influence on the efficiency of the system [8–12]. However, there are no specific guidelines with focus on grouting for horizontal geothermal installations either [13]. And in most cases, this involves the use of vertical probe systems. Consequently, many systems are dimensioned inadequate. For safety reasons, very shallow geothermal installations are dimensioned mostly too big, by just using a rule of thumb. In cases of space scarcity, this can be an evitable knock-out criterion for these very shallow geothermal systems. However, in order to match the dimensions of these geothermal systems according to the geothermal potential of the ground environment, the soil properties and the grouting characteristics with regard to heat transport must be known.

* Corresponding author.

E-mail addresses: hans.schwarz@fau.de (H. Schwarz), jlin@unistra.fr (J. Lin), david.bertermann@fau.de (D. Bertermann).

<https://doi.org/10.1016/j.renene.2024.120664>

Received 4 June 2023; Received in revised form 10 May 2024; Accepted 13 May 2024

Available online 18 May 2024

0960-1481/© 2024 The Authors. Published by Elsevier Ltd. This is an open access article under the CC BY license (<http://creativecommons.org/licenses/by/4.0/>).

For convenient recommendations on the feasibility of very shallow geothermal installations information of the soil properties thermal conductivity, water content, bulk density and soil type are needed [8,10,14,15]. Such information could be delivered by geothermal potential maps [6,16]. But these potential maps cannot substitute detailed on-site investigations.

By applying Electrical Resistivity Tomography (ERT) measurements within this study a non-invasive investigation method is tested for examinations on the basic parameters that are decisive for the thermal properties. In comparison to selective drilling points, by measuring ERT sections, a large area can be covered for a continuous soil screening. Formerly self-potential measurements were performed to examine deeper geothermal systems [17,18]. Generally, ERT measurements are influenced by several physico-chemical soil properties [19,20]. Particularly, ER is very sensitive to water content of soil [20–25], whereby the groundwater level can be additionally detected if present. Another influencing parameters are soil texture and bulk density, and even if they are not as decisive as water content these parameters can conversely be derived from ER [26]. Moreover, temperature is influencing the ER measurement results [27–30], which is analysed in this study and reflected in the temperature correction models [19,31]. Since the same soil physical properties affect the electrical resistivity as well as the thermal conductivity of soil [32–35], ERT data can be used to derive soil thermal parameters [36–40] as key parameters for defining a geothermal potential.

However, until now for investigations of the ground thermal properties around very shallow geothermal systems, ERT measurements have been used rarely [28,41–44]. Just a few investigations regarding very shallow geothermal systems are focusing on heat propagation [45–47]. And none of these investigations were applied to an earth air-heat exchanger – system (EAHE), which is an air conveying GSHE buried in very shallow depth like other very shallow geothermal applications [48–54]. As it applies for all GSHE installations, the ground is utilized as heat sink or heat source. Hence, its energy performance depends on the physical-thermal properties of the surrounding material [8,9,55].

Thus, within this study the soil and grouting material surrounding of a EAHE as a GSHE installation was investigated with ERT measurements. The objective was on the one hand to categorise the soil texture and the grouting material in terms of ER and on the other hand to evaluate the effect of variable grouting materials, seasonal variation of soil temperature and the running of the EAHE on the measured ER values. At the same time the investigated effect of a changing soil temperature assesses the robustness of the ERT measurement. To do so the ERT measurements were carried out at spring and winter seasons, and at each time with running and shutdown of the EAHE system. The measurements were carried out on a EAHE test site in Strasbourg France, where different grouting materials are installed. The fact that the different grouting materials at the site have an influence on the energy performance of the EAHE system has already been investigated [8,9]. Lin et al. [55] have already studied the impact of soil moisture on the energy performance of this system and also the influence of rainfall events [56]. So, the effect of different parameters on the energy performance of the very shallow geothermal system was already investigated and the main task in this study was to measure these influencing parameters in the vicinity of a very shallow geothermal installation with a preferably fast and non-invasive method. At the same time, soil temperature is shown as an interfering factor that users should definitely take into account when interpreting ER.

Such an investigation method should enable recommendations on the determining soil factors for an estimation of feasibility and the dimensioning of very shallow geothermal systems. The advantage of this method is the performance directly on-site in a fast and cost-efficient way. Due to the fact that, the non-invasive ERT measurements can also be applied after the installation works, also an inspection of the added grouting material is possible.

2. Research methodology

2.1. Presentation of the geothermal site in Strasbourg

The EAHE site of this study is located in France at the Civil Engineering department of University of Strasbourg. The EAHE is divided into three segments that are associated with a different groutings as coating soil material: (1) fine sand; (2) a mix of fine sand and bentonite (10 %), (3) and natural soil backfill composed of gravel-clay mixture, respectively (Fig. 1). Within the second segment, the same fine sand has been used in the first segment of the EAHE as the coating soil. The sand used within the sand coating segment is also implemented as bedding material within all segments.

The heat exchanger surrounding corresponds to the rectangular excavation form, which is 1.2 m wide and 0.55 m high, where the lower 15 cm are filled with the bedding sand and the upper 40 cm with the coating material (Fig. 1). The heat exchanger pipe has a regular slope of 2 %, which is imposed to avoid the stagnation of condensation water. For that reason, installation depth is increasing by a few decimetres along the system (Fig. 1). Within the sand segment the pipe coating starts at an average of 0.53 m below surface. The coating starts at a depth of 0.72 m (average) regarding the second segment and at 1.00 m depth (average) within segment 3.

2.2. Information of soil texture

In order to analyse the surrounding soil layers around the GSHE, within this study a soil probing was carried out in the EAHE area of the second segment while the installation works took place. In the investigated spot the sand-bentonite coating starts at 67 cm depth, which is due to the more anterior position less than the average of 72 cm for this segment. Within a depth from 93 cm until 127 cm the sand bedding was incorporated, below which the natural soil is following. It has to be considered, that this ascertained installation depth of the sand beddings lower bound is significantly deeper than in theory. This shows possible differences towards the installation scheme of [8] and potential thicker bedding sand layers.

A granulometric analysis was performed to obtain the grain size distribution of the different implemented soil types as grouting materials that are already investigated with regard to their thermal properties [8,55]. Sieving of dry soil sample was carried out for each soil type. An additional sedimentation measurement was performed for the mix of sand and bentonite due to the importance of its content of fine particles (grain size < 0.1 mm) (Fig. 2).

Beside the soil probing in the course of the EAHE system installation an additional soil probing in the area, of initial field conditions (area of ERT measurement section 2) was carried out. This probing was performed with a drill hammer.

The soil profile of initial field was recorded until a depth of 1.7 m, because with the used probing application a deeper penetration was not possible due to the gravel (Fig. 3). The topsoil is just 0.05 m deep followed by a soil layer composed of gravel-clay until 0.7 m depth. Subsequent, there is loamy soil down to 1.2 m with some coarse gravel fragments, which also might be due to a collapse of the borehole. From 1.2 m until 1.4 m a pure clay is following. The lowest recorded layer was gravel with sand that reached up to 1.7 m.

2.3. Seasonal soil conditions

To get an indication of a seasonal impact within the relevant depth of very shallow geothermal installations by measuring the ER, the ERT measurements were carried out in May 2019 and February 2020. The soil parameters that are seasonal are soil moisture content and soil temperature.

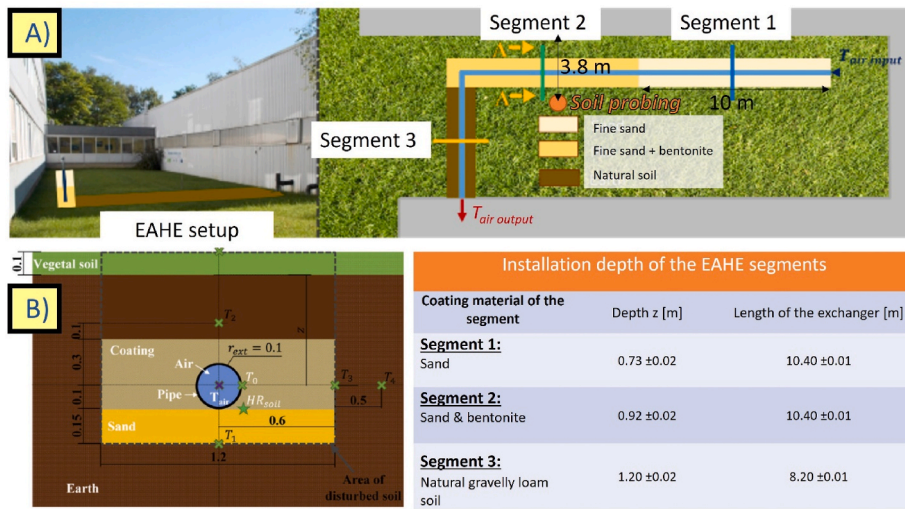


Fig. 1. Test site with the EAHE installation at the Civil Engineering department of University of Strasbourg. A) View over the test site on the left and an aerial perspective on the right and B) slice of the installed EAHE system with the dimensions of the pipe, the coating material and the sand bedding with a table of the installation depth of each segment (adjusted from Ref. [8]).

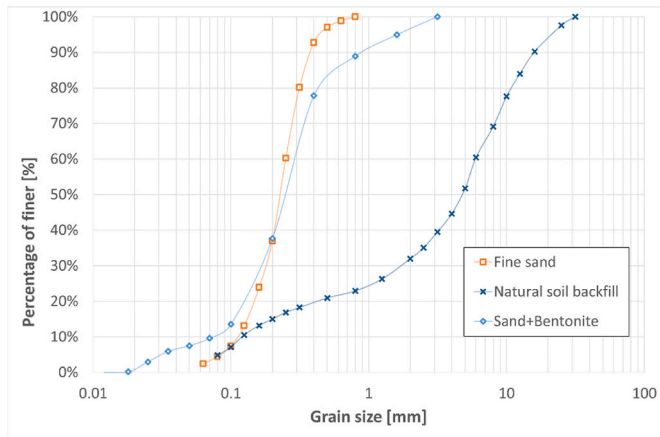


Fig. 2. Granulometric analysis of the different used soil materials.

2.3.1. Soil moisture seasonal variation

To describe this seasonal variation of soil moisture this parameter was monitored over several years (Fig. 4). Over this period soil moisture was volatile around 15 Wt-% until 25 Wt-% in winter and spring, depending on precipitation quantities, and dried down to 9 to 10 Wt-% at the end of summer. This displays the situation in the installation depth of the heat exchanger. Within deeper or more shallow soil layers, this seasonal influence has a correspondingly greater or lesser effect.

In order to avoid great soil moisture difference at the test site for a focus on temperature variability, the summer period was avoided and the two chosen test seasons are winter and spring.

2.3.2. Soil temperature seasonal variations

In addition to soil moisture, soil temperature is the simplest and most direct indicator of seasonal changes. This parameter was also monitored in the installation depth of the heat exchanger. In case of this parameter, no variations occurred between the different segments. As shown in Fig. 5 on the dates in early February, soil temperatures were around 8.0 °C. The soil temperatures in May were then already significantly higher at 13.0 °C.

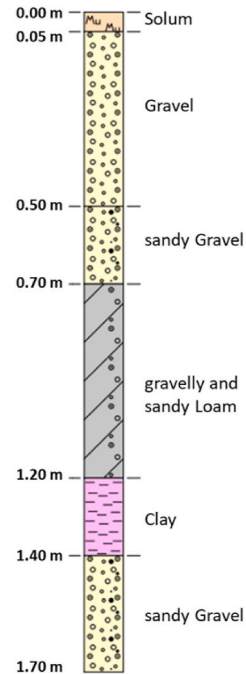


Fig. 3. Soil profile of the initial field conditions determined by a drill hammer investigation within the area of ERT measurement section 2.

2.4. ERT measurement and data process

2.4.1. ERT measurements

Within this survey the ERT sections were measured with the ‘4point light’ resistivity meter of LGM—Lippmann Geophysical Equipment and the GeoTest software developed by Geophysics—Dr. Rauen within two field campaigns in May 2019 and February 2020. Each ERT section (Fig. 6) was measured twice per field campaign: the first time was carried out on the first day while the EAHE system was still running and the second time was performed the day after while the heat exchanger system was shut down. Since the system was shut down in the evening after the first measurements, the soil temperatures around the EAHE system had a recovery time of at least 15 h.

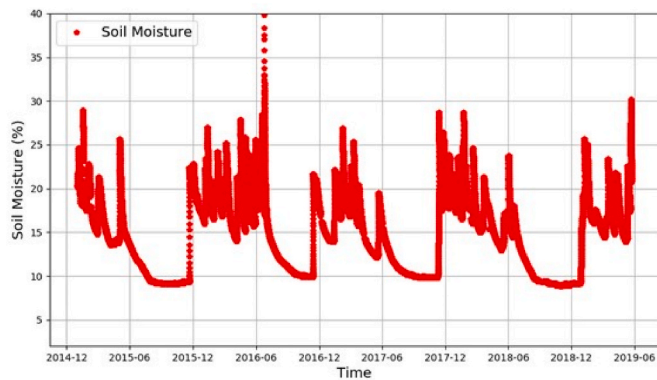


Fig. 4. Soil moisture [in Wt-%] trend over several years within the fine sand segment of the EAHE installation (segment 1).

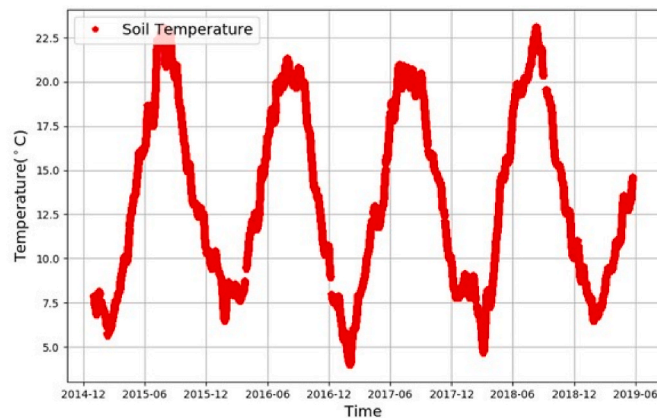


Fig. 5. Soil temperature trend over several years at the depth of the EAHE installation.

By using the ‘4point light’ device, the ER or rather the electrical conductivity of the underground was determined in form of 2D-ERT profiles. As shown in Fig. 6, two sections (S1+S2) were measured with 80 electrodes and a spacing of 50 cm each. S1 was performed upon the heat exchanger in a distance of 1,2 m to the building. S2 serves as a reference on the original soil composition and was also measured parallel to the building with a distance of 3.75 m. S2 keeps a parallel distance of 2.55 m with S1. The heat exchanger area underneath S1 starts between electrode 8 and 9 (around the 4th meter) and turns to the hall of the Civil Engineering department after the second segment between electrode 51 and 52 (around the 25th meter).

Furthermore, three short sections S3, S4 and S5 were measured in a width of 6.0 m with a spacing 20 cm. The aim of measurements of these 3 short sections is to reveal the different EAHE grouting materials. However, due to the proximity of the heat exchanger to the building, the investigated zone (surrounding soil of the heat exchanger) could not be recorded in its entirety. Moreover, the penetration depth of these short sections was not sufficient for a proper identification of the focused layers at the EAHE installation depth. Taking this into account, these short sections were not used for further investigations of this study.

The measurements were carried out using the Wenner array [57–59] because it is less sensitive to noise, especially near buildings, and it enables reasonable results regarding horizontal soil layers. The set frequency was 4.16 Hz.

2.4.2. ERT data processing

In the aftermath of the measurements the raw resistivity data was processed to determine the effective ER. Therefore, data inversion was

performed with the Res2Dinv software by Aarhus GeoSoftware previously Geotomosoft.

In order to have a cohesion in the evaluation of soil ER values, some corrupted datapoints were exterminated before the inversion process. This step concerns especially the S1 measurements which are affected by presence of the vertical air input tube of the EAHE system at the beginning position of the first segment.

A refined model with a grid width = 0.5*electrode spacing was used for inversion process. Moreover, a robust inversion method with the complete Gauss-Krüger computation was carried out for several iterations. Regarding the data investigation of this study the 5th iteration of each inversion process was used. For graphical depiction of the ERT results the same contour intervals were applied.

2.4.3. ERT data analysis

For a further detailed investigation of the ER values of both sections S1 and S2, the inversion data of the 5th iteration was exported to an Excel-format file. Within this analysis, ERT data of 9 depth layers were used. With the aim to evaluate the ER values with the information of different soil textures, these 9 depth layers were superimposed by different soil domains of the EAHE site as shown in Fig. 9. 4 types of soil and grouting domains were considered in the analysis: Topsoil, Coating Layer, Bedding Layer, and Bottom Soil, which is the in-site soil beneath the installation.

Thereafter, ER values were classified by soil domains and analysed. This classification was applied to data of S1 section but also to that of reference section S2 for comparison purpose. The average value of ER in each soil domain was used in further comparison analysis. To avoid edge effect, ER values near the transient area of two different segments were not included in the calculation of the average values (Fig. 7).

To improve comparability of ER values the raw resistivity values are corrected by temperature (T) according to Refs. [19,31]. Therefore, the reciprocal value of ER, the EC values (σ_T) are processed as the following equation (1 + 2).

$$\Sigma_{25} = f_T \bullet \sigma_T \quad (1)$$

$$f_T = 0.4470 + 1.4034 \bullet e^{-T/26.815} \quad (2)$$

In the case of this study, the used temperature values are $T = 8 \text{ }^\circ\text{C}$ for February and $T = 13 \text{ }^\circ\text{C}$ for May, since these temperatures were monitored in the depth of the heat exchanger.

However, it has to be considered that the used temperatures for correction refer to soil temperature in installation depth of the EAHE system. A gradual temperature profile was not taken into account.

3. Experimental results

3.1. Results of ERT measurement

To show the distribution of the ER [Ω^*m] below the subsurface, the inverted results of the ERT measurements, performed within different seasons upon the EAHE system (Fig. 8), and of the reference measurement (Fig. 9) are displayed. By applying an ERT section length of 39.5 m a maximum penetration depth of around 6.8 m was achieved.

The left side of the depicted profiles is determined by the placement of the first electrode and the measurement device, which corresponds to the northern end of the sections. Contour intervals for ER are determined logarithmic with a start value of 20 Ω^*m and a multiplier of 1.275.

Regarding S1 (Fig. 8), there are specific ER values on top of the profile that vary from 40 Ω^*m to above 100 Ω^*m . Below 0.5 m depth ER rises in parts clearly above 140 Ω^*m . This depth of around 0.5–0.7 m corresponds also to the top of the grouted segments. Within the depth of the EAHE installation, the ER shows distinct variabilities between 140 Ω^*m and 350 Ω^*m .

To verify the influence of the EAHE installation, the results were

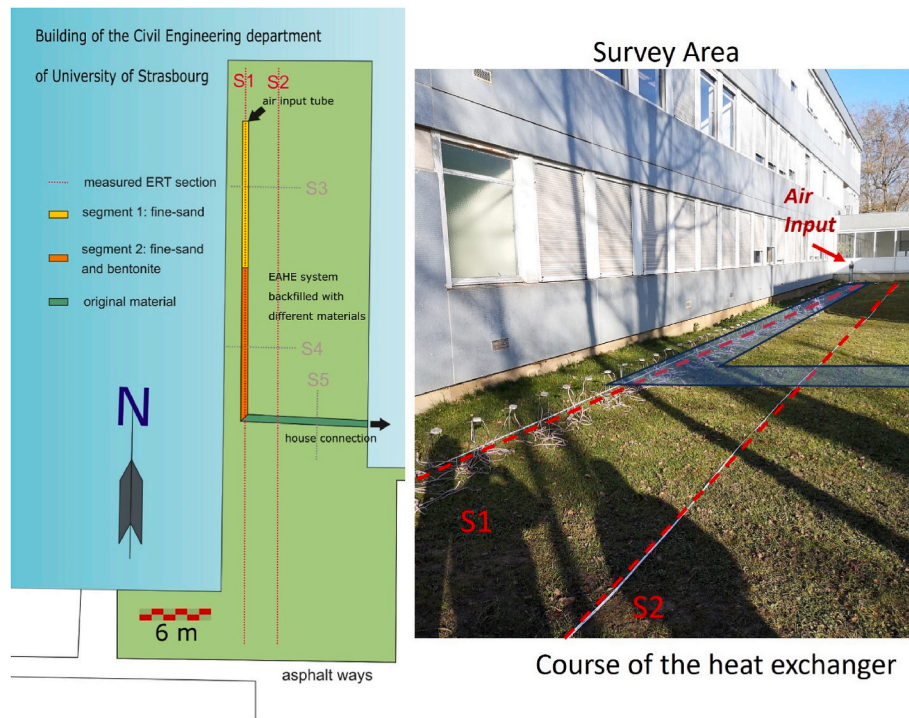


Fig. 6. Scheme (left) and picture (right) of the survey area at the Civil Engineering department of University of Strasbourg. Position of the electrical resistivity (ERT) measurements S1 and S2 on the horizontal heat exchanger (EAHE). Measurement application for the measurement of S2.

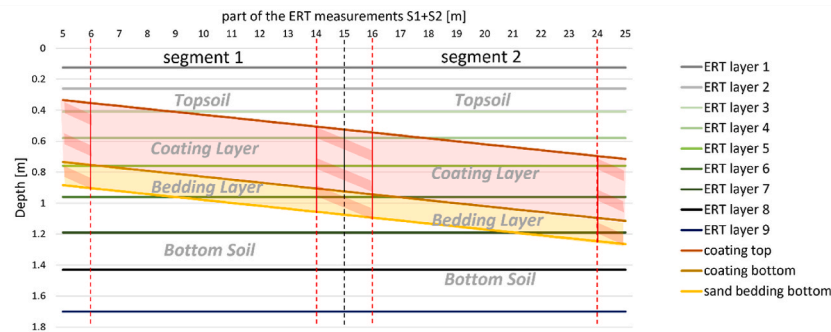


Fig. 7. Depths of the measured ERT data layers, that are used for further analysis and the depths of the EAHE installation over the distance of segment 1 and segment 2 taking into account the omitted border areas. The cutting lines “coating top”, “coating bottom”, and “sand bedding bottom” define the exact affiliation of the data points on each ERT layer.

compared to the undisturbed conditions measured within S2 (Fig. 9). The ER values of the topsoil of S2 are around 40–80 Ω*m and with that they are in a similar range compared to the topsoil resistivities of S1. Moreover, the ER within this topsoil in S2 is more evenly distributed than that in S1. This more homogeneously distributed and less variation ER values are also observed for the soil layers below the topsoil. Overall, the highest ER values within greater depths are around 300–500 Ω*m.

3.2. Comparison of initial field section S2 and the EAHE installation section S1

To enable an accurate comparison between the initial field section S2 and the EAHE installation section S1 as well as between both domains of grouting materials (segment 1 and segment 2), the ER values at different positions were averaged regarding the different domains as described in Fig. 7 and corrected for temperature by using equations (1) and (2).

It should be considered that the two segment zones are also applied at the reference section S2 for the purpose of comparison with S1. There is not a real soil difference between these two segments at section S2.

Table 1 shows average ER values at the two EAHE grouting segments for section S1 and section S2. Each average value is calculated from the 4 ER values derived from the 4 measurements performed on the same zone (2 at May and 2 at February).

It becomes clear that the ER values within the relevant depth are generally higher within the EAHE area than within the natural soil conditions. This is particularly evident in the first segment, where differences of $\Delta = 88.9 \Omega \text{ m}$ and $\Delta = 95.5 \Omega \text{ m}$ occur within the Coating Layer and the Bedding Layer respectively. Regarding the second segment the highest difference shows up in depth of the Bedding layer ($\Delta = 42.8 \Omega \text{ m}$), and the differences within the other layers are less than $\Delta < 22 \Omega \text{ m}$. Hence, the ER values of the second segment in S1 correspond more to the natural state represented by S2. Concerning the Bottom soil, which is the same soil type for both S1 and S2, the ER values are very similar between the two sections. For example a little difference of 5.8 Ω m is observed at segment 1 between S1 and S2.

Thus, the result reflects a disturbance of the upper three layers due to the EAHE installation and the Bottom soil layer corresponds approximately to the reference values.

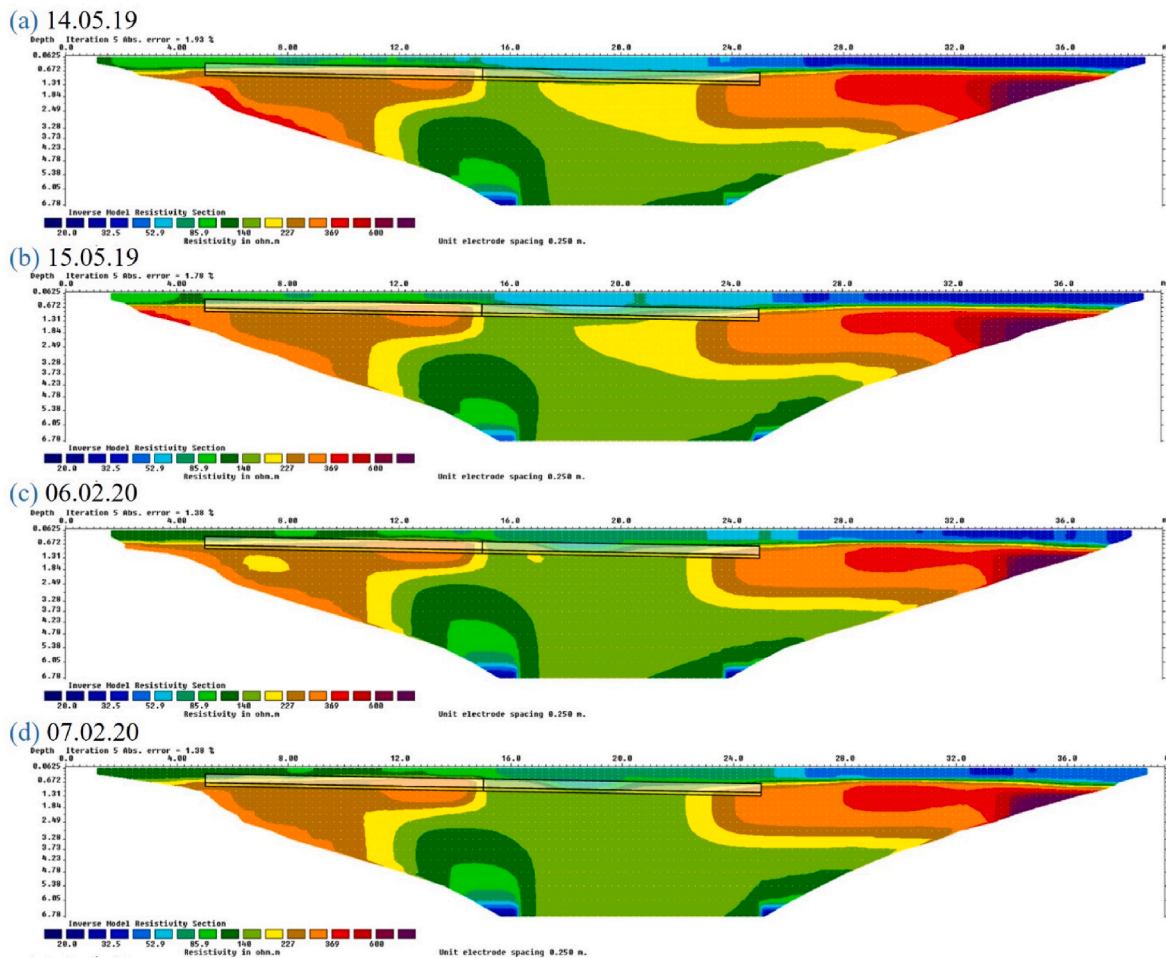


Fig. 8. ER distribution of the measured section S1 upon the EAHE system, while the heat exchanger system was running (14.05.2019 (a); 06.02.2020 (c)) and after shutting down the heat exchanger system (15.05.2019 (b); 07.02.2020 (d)). The ER values are according to the 5th iteration of the inversion process. Both grouting segments (left: fine sand; in the middle of the section: fine sand and bentonite) with the underlying sand bedding are delineated by black lines.

3.3. Comparison of coating segments at EAHE installation section S1

For defining the influence of the different coating materials in first instance the difference between segment 1 and segment 2 regarding the ER values of S1 must be highlighted (Fig. 10). There, the Topsoil ER is quite stable in comparison with the other three layers (Coating Layer, Bedding Layer, Bottom Soil). Within the other three layers, a significant shift from segment 1 to segment 2 becomes apparent.

3.4. Impact of seasonal soil temperature variation

For analysing the impact of the changing soil conditions by season, the ER values of the February ERT measurements are compared with the values from May (Fig. 11 and Appendix). As a background information the seasonal soil temperatures for the Coating Layer are given (February: 8 °C; May: 13 °C). Corrected ER values decrease due to a correction at temperatures below 25 °C. With the temperatures used correction factors of $f_{T_{may}} = 1.31$ and $f_{T_{feb}} = 1.49$ were determined for EC. With regard to the resistivity values, this 5 °C temperature variation results in a difference of approx. 18 Ω m when applying an initial value of 200 Ω m, which represents a difference of almost 10 %. This goes in conformity with empirical linear approximations of 1.8–2.2 percent change in bulk electrical conductivity per degree C (Hayley et al., 2007).

Regarding the uncorrected results for Section S1, the highest differences between February and may (mostly above 20 %) occur within the upper two Layers (Topsoil and Coating Layer). Whereby this effect is

more distinct within the Segment with fine sand and bentonite (>23 %). In this case the seasonal deviations within the Bedding Layer and the Bottom soil are less than 6 %. For Section S2 on the reference area, the uncorrected results also show the same tendency even more clearly with distinctly higher deviations within the Topsoil and the depth of the Coating Layer (>26 %) and less differences in the deeper Layers (<16 %).

After the application of the temperature correction there is a shift in deviations between the layers examined. Regarding the Section S1, that represents the ERT measurement directly upon the EAHE system, now the least deviations occur within the Coating Layer (<4.7 %). Concurrently, the Topsoil above and the other two Layers below show higher seasonal effects now (Topsoil: 9.7–11.3 %; Bedding Layer: 14.8–16.0 %; Bottom Soil: 18.9–19.8 %). In contrast to the uncorrected results, there is no significant difference between both Segments to be found.

Within the corrected results for Section S2, the trend that the second layer has by far the lowest values is not so clear. In this case the deviations between May and February vary more. Still, within the depth of the Coating Layer and the Bedding Layer there are lower difference by average (Coating Layer $\Delta_{av} = 17.2$ %; Bedding Layer $\Delta_{av} = 8.2$ %) than above (Topsoil: $\Delta_{av} = 22.1$ %) and below (Bottom Soil: $\Delta_{av} = 26.4$ %). But in this instance the least deviations are within the Bedding Layer and not within the Coating Layer as determined in Section S1.

Regardless of the temperature correction and the respective ERT measurement (S1, S2), the measured ER values in February are almost always higher in the top two layers and lower in the bottom soil than in

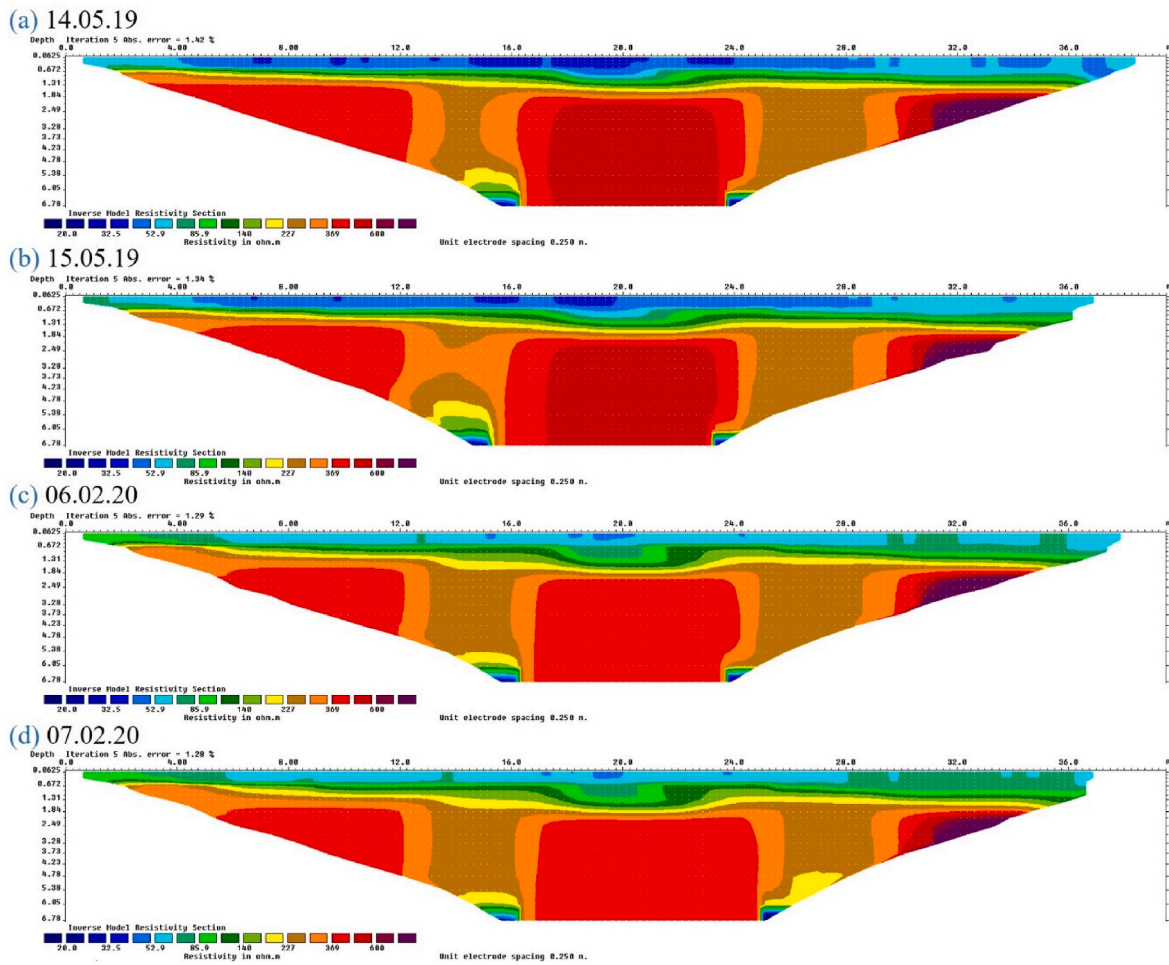


Fig. 9. ER distribution of the measured section S2 as reference while the heat exchanger system underneath S1 was running (14.05.2019 (a); 06.02.2020 (c)) and after shutting down the heat exchanger system (15.05.2019 (b); 07.02.2020 (d)). The ER values are according to the 5th iteration of the inversion process.

Table 1

Temperature corrected average ER values of the four representative layers for both segments 1 + 2 and for all four performed measurements of S1 and S2.

Section	Layer	Average ER values [$\Omega \cdot m$]	
		fine sand coating Segment 1 (6–14 m)	fine sand + bentonite coating Segment 2 (16–24 m)
S1 (above EAHE)	Topsoil	70.72	48.17
	Coating layer	141.54	69.06
	Bedding layer	203.56	117.50
	Bottom Soil	194.82	129.49
S2 (reference)	Topsoil	37.92	34.71
	Coating layer	52.65	58.57
	Bedding layer	108.06	74.69
	Bottom Soil	200.65	107.36

May. By applying the temperature correction there is a reversal of values just within the Bedding Layer. For this layer ER values are throughout higher in February before the correction and after the correction the ER values are higher in May.

3.5. Impact of EAHE system running

To examine the impact of the running EAHE system, the data of the first measurement day of each measurement campaign, when the very shallow geothermal system was still running, is compared with the similarly performed ERT measurements on the next day, after the EAHE system was shut down in the evening before. Moreover, to evaluate the

influence of the system, the differences between the first and second day were considered for both Sections, S1 and the reference S2 (Table 2). If an effect of the EAHE system is present, it should occur in S1, whereas only natural noise can be detected in S2.

Regarding the difference between both measurement days, the absolute changes are very small ($\Delta < 9.4 \Omega m$). Within installation depth (Coating Layer) of S1 the differences in Segment 1 with the fine sand coating are distinctly higher than the change of ER within Segment 2 (Coating Layer S1 $\Delta_{fs} = 5.0 \%$; $\Delta_{fs + b} = 1.3 \%$). Also, in comparison with the measured ER in Section S2 the change are less within the first Segment area. But in the area of Segment 2 of the Section S2 measurement, there are also deviations of more than 5 %, although the absolute

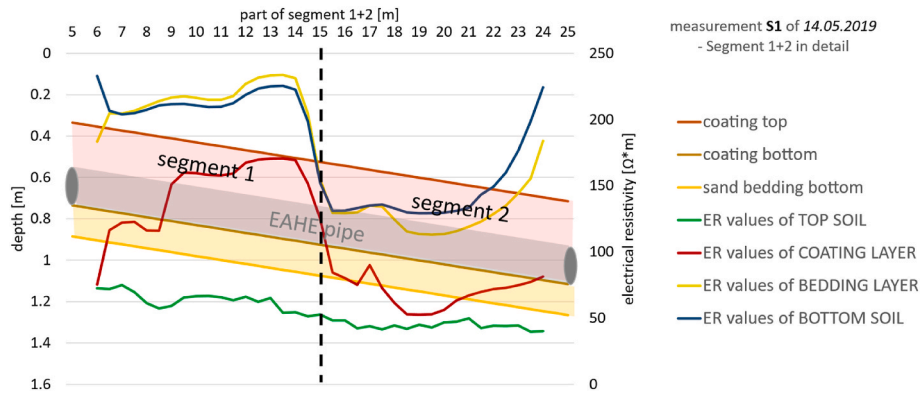


Fig. 10. ER results corrected by temperature and merged for each layer of the S1 measurement of may in the range of the investigated coating layer segments of the EAHE installation and their respective depth.

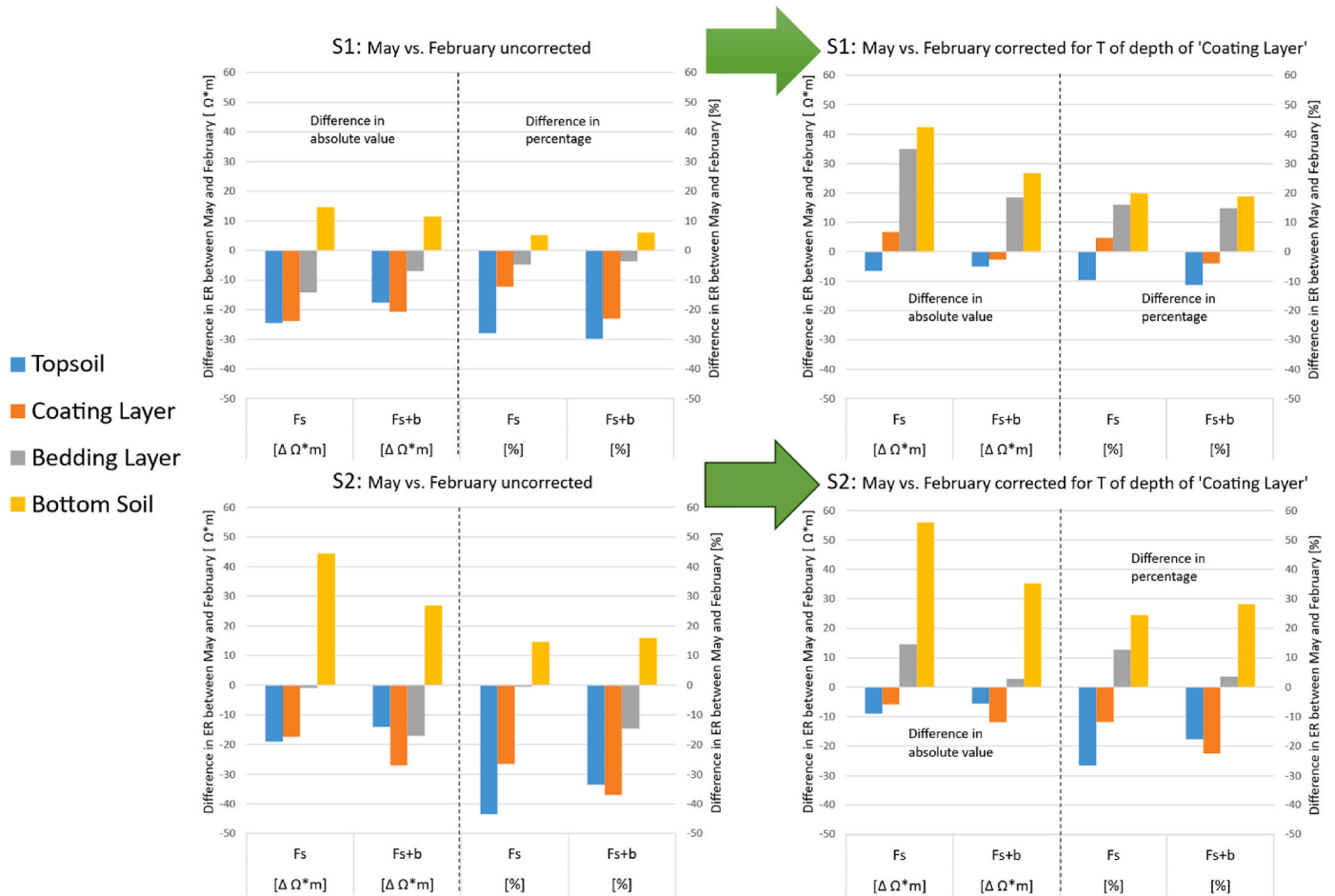


Fig. 11. Comparison of February and May ER values once corrected by temperature and once not, to highlight the seasonal impact in the course of both measured ERT sections (S1+S2).

value is a little bit less.

It has to be considered, that the performed temperature correction has no influence on the result in this case, since in this data analysis the differentiation of ER values is always made between measurements of the same measurement campaign (February or May). Thus, the compared ER values in each case are corrected with the same correction factor.

4. Discussion

Soil conditions and the thermal characteristics of the grouting material are essential for the performance of near-surface geothermal energy. With variation in soil properties and grouting material the needed space for a very shallow geothermal installation to cover a distinct demand for heating or cooling is affected. Within the study of Lin et al. [55] the impact of water content on the energy performance of an EAHE was already investigated. Furthermore, the impact of the different grouting materials was analysed [8,9].

Table 2

Mean differences as absolute values of ER values [$\Omega \cdot m$] corrected by temperature and as differential in percentage between first day and second day measurements to showcase the impact of EAHE system within S1 in comparison to S2.

Segment	Impact of EAHE		Background noise	
	Results for Fs and Fs + b for S1 (running – not running)		Results for Segments Fs and Fs + b for reference S2 (first day – second day)	
	Fs [$\Omega \cdot m$] (%)	Fs + b [$\Omega \cdot m$] (%)	Fs [$\Omega \cdot m$] (%)	Fs + b [$\Omega \cdot m$] (%)
Topsoil	-3.9 (5.8 %)	-2.0 (4.2 %)	-1.3 (3.5 %)	-1.4 (4.2 %)
(Depth of) Coating Layer	-6.9 (5.0 %)	0.9 (1.3 %)	-1.4 (2.6 %)	-3.2 (5.7 %)
(Depth of) Bedding Layer	-5.2 (2.6 %)	3.8 (3.1 %)	0.1 (0.1 %)	1.2 (1.5 %)
Bottom Soil	-1.8 (1.1 %)	2.3 (1.6 %)	4.3 (2.1 %)	9.4 (7.7 %)

But is it still possible to check afterwards whether the correct material was used? In order not to cause any damage, only non-invasive measuring methods like ERT measurements can be used. To define relevant soil properties for very shallow geothermal potentials ERT measurements can be used as a tool. However, ERT measurements determine the electrical conductivity and the soil properties are 'only' derived from the measured results. If the ERT measurement is affected by varying influencing parameters which are not taken into account, this can lead to incorrect derivations or misjudgements. It is therefore essential to take a close look at the influence of the changing parameters with season on the ERT measurement to be able to make the right conclusions in the end. The following discussion points mainly deal with the determination of the soil and grouting material and the influence of temperature from different sources to analyse the weaknesses and possibilities of the used methodology.

4.1. Classification of soil and of the grouting material by ER values

In general, finer-grained soils exhibit lower ER than coarse-grained soils [21,29]. Regarding the investigated soil in this study, besides the solum the natural soil profile consists almost entirely of soil layers characterised by gravel with only few fine-grained horizons. The granulometric analysis of a gravel layer exhibits that more than 60 % of the natural soil backfilling material consists of gravel and a total of 20 % correspond to grain sizes of medium and coarse gravel ($\varnothing > 10$ mm). Due to the original coarse soil material ER values are rising distinctly over 100 $\Omega \cdot m$. According to the GGU [60] saturated sand and gravel are around 50–200 $\Omega \cdot m$. Just moist gravel has already values $> 1000 \Omega \cdot m$. With values above 200 $\Omega \cdot m$ throughout the profile below the installation depth it is clear, that the original soil texture is very coarse.

In contrast to the coarse-grained soil textures, within the EAHE installation the added coating material defined as a fine sand has no gravel content and in the case of segment 2 additionally a small amount of fine-grained soil material (≈ 10 %) comes on top. For silt soil for example, a range of 20–100 $\Omega \cdot m$ is given as a rough recommendation. This is mainly due to the sensitivity of the ERT measurements in relation to the soil water content, which is generally higher in finer-grained soils [20,21,25].

Hence, it would be expected that the ER in Segment 2 (fs + b) would be lower than in Segment 1 (fs) and the values in the whole area of the grouted GSHE would be lower than those in the same depth of the reference measurement S2. This rough assumption is reflected in the results of the geoelectric investigation (Figs. 10 and 11). One might have expected that a layer with bentonite would have even lower ER values than such a gravelly loam like the initial soil. But in this case the amount (≈ 10 %) is not sufficient to obtain clay specific ER values that are below 20 $\Omega \cdot m$.

Regarding the ERT measurement itself, the performed electrode spacing of 0.5 m should ensure an optimal adapted spatial resolution, since Dumont, Pilawski, Hermans, Nguyen and Garré [23] also tested different electrode spacings and have recommended an electrode spacing of 0.5 m for the best possible resolution at the investigated depth. Although, characterisation of ERT results must be taken with caution [61].

For the further discussion it has to be considered, that in partial areas this ascertained installation depth of the Sand Beddings lower bound can be deeper than in theory. At the soil-probing point within segment 2 a divergence was found. Whereas the theoretical thickness of the bedding sand layer should be 0.15m, the actual measured thickness is about 0.34 m [8].

4.2. Comparison between initial field conditions and the geothermal installation

It was found that the ER values within the installation depth are generally higher within S1 than in the initial field conditions of S2. It is unclear whether the installed heat exchanger pipe itself has an influence on the ER values of the Coating Layers of S1. This could possibly also increase the ER of S1 somewhat.

In detail it has to be considered, that the natural soil profile shows a loamy layer with a small subjacent clay layer in the same depth at which the EAHE system was installed (Fig. 4). This explains that the ER values in the reference measurement S2 in the depths of Coating Layer and Bedding Layer (Table 1) correspond to ER values of loamy or silty soil. ER values only increase to 'gravelly' values in the Bottom Soil Layer. The ER values of the natural soil (S2) at the depth level of Coating Layer are therefore converging to the values of the coating material with the bentonite addition in Segment 2 of S1. Hence, the ER values of the grouting material of the second segment correspond more to the natural state, due to the loamy and clayey layers present within installation depth.

Since the fine-grained component is missing in the grouting material (Coating Layer) of Segment 1 as well as within the Bedding Layer of both Segments, higher ER values within section S1 are significant in these domains.

With regard to the differences between all four investigated Layers, the result reflects a disturbance of the upper three layers, ascertained by elevated ER values, due to the EAHE installation. But the Bottom Soil Layer corresponds approximately to the reference values.

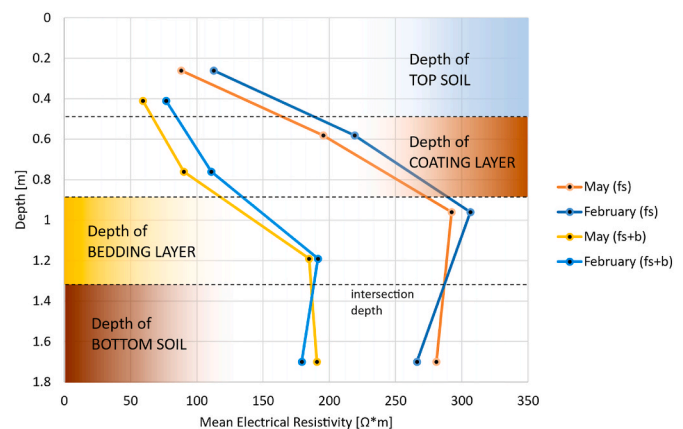


Fig. 12. Not corrected mean ER values. Profiles of Section 1 (above the EAHE installation) for February and May and for each Segment respectively.

4.3. Comparison of coating segments

The measured ERT section S1 (Figs. 10 and 12) shows, that the two grouting segments of only fine sand and fine sand with bentonite can be distinguished, clearly.

With regard to the average ER values for the investigated Layers of Section 1 (Fig. 12), ER of Segment 1 with only fine sand is significantly and throughout higher than the ER values of the Segment 2 with fine sand and bentonite. This result is still true also a small shift between both segments could already occur because the represented domains are descending with the slope of the EAHE installation.

Taking the reference measurement S2 into account it shows clearly that the deviation within the Coating Layer must be due to the different coating materials, because within the same depth in S2 the ER values are even lower than in Segment 2 of S1 and they are very steady.

The difference between both installed grouting materials was to be expected, because the addition of a fraction of fine grains to a pure sand. Although the bentonite addition is just around 10 %, it changes its physical soil properties and primarily the water retention capacity [62]. And due to the sensitivity of ERT with respect to water content [20,21, 25], this change in soil texture could have been resolved very clearly.

The difference between both grouting segments is most evident in the Coating Layer ($\Delta_{\text{Coating Layer}} = 51.1 \%$) and the Bedding Layer ($\Delta_{\text{Bedding Layer}} = 42.2 \%$), but there are also differences around 30 % in the Bottom Soil. With that the difference in the Bottom Soil almost reaches the same proportions as the Layers of the installed EAHE system. Regarding the Topsoil the absolute difference ($\Delta_{\text{Topsoil}} = 22.6 \Omega \text{ m}$) is lower than within the other Layers and on the contrary to all deeper layers no distinct change between both segments is detected (Fig. 12).

It seems that the impact of the different soil textures considering the respective grouting materials also affects the surrounding ERT results. Regarding the mean ER values in Topsoil, generally they are also higher than in the reference area and they decrease gradually from segment 1 to segment 2, although the reference indicates a steady state under natural conditions. Although, there is no significant transition between the ER of both segments in the Topsoil, it may be, that due to these different grouting materials or rather soil textures of the EAHE Coating Layers, soil of the layer above is also affected. The influencing factor could be the fact, that the soil material with a small amount of bentonite incorporated in segment 2 has higher water-holding capacity which may influence also saturation of the Topsoil Layers.

This influence of the Coating material on the surrounding layers is even more pronounced in the Bedding Layer and Bottom Soil, where ER values are distinctly higher in the area of Segment 1 than in the area of Segment 2 (Fig. 12).

Although, the Wenner array has generally a relatively low noise contamination, sometimes the spatial resolution is reduced [58]. Dumont, Pilawski, Hermans, Nguyen and Garré [23] have also stated a shift of the ER results to larger depths of around 0.5 m at an investigation depth similar to the installation depth of the EAHE system. Thus, it is therefore possible that, in addition to the influence of the modified soil texture above, ER processing also has an influence on the lower layers.

With regard to the reference ERT measurement S2, where the same data accumulation was carried out, no significant changes in the Topsoil Layer were achieved. In S2 first notable differences occur in depth of the Bedding layer and become distinct in the Bottom Soil layer. Thus, the shift of ER values in the upper two layers between Segment 1 with fine sand and Segment 2 with fine sand and bentonite is unambiguously due to the different Coating materials, whereas the shift beneath the installation within the Bottom Soil can also be partly attributed to pre-existing natural conditions.

Nevertheless, the different grouting materials show their influence because the change of ER in the Bottom Soil layer is very clear at the transition between both segments (Fig. 12).

Furthermore, it is shown that differences within grouting material can be detected, which enables the possibility for controlling the

backfilled grouting material of a very shallow geothermal system after installation by using non-invasive ERT measurements. The right grouting material may be crucial for an increased energy performance and with that a diminution of a needed tube length [8].

4.4. Seasonal temperature variation

Regarding the results compared between February and May, the influence of soil temperature on ER cannot be denied. In order to determine the influence of the seasons, the corrected and not corrected measurements from February were compared with those taken in May.

Regarding the not corrected ER values (Fig. 11), the contrast between February and May is more significant within the near surface layers and the differential decreases with depth. This is true for both measured sections (S1 and S2), although this trend is more pronounced in the reference measurement S2. Thus, within the Topsoil and the Coating Layer there are the highest percentage deviations of ER between February and May, whereas the deviations in the depth of the Bedding Layer and the Bottom Soil vary less. This also applies to the absolute difference of ER, although this trend is not as significant then, due to the fact that the measured ER for the deeper layers is at higher values.

As the year progresses, soil temperatures change and this change of temperature decreases with depth [27,63]. Hence, this measured ERT variation between February and May is generally consistent with the seasonal temperature spread decreasing with depth. The variations of ER are highest in Topsoil and decrease with depth.

It should be noted, that the sign of the differentials is reversed in the Bottom Soil layer (Fig. 13). Thus, the measured ER within the depth range of the EAHE installation (Topsoil, Coating Layer, Bedding Layer) are consistently higher in February than in May. But within the Bottom Soil Layer this changes and ER are higher in May.

That within the cold season higher ER within the near surface layers occur correspond to the general context that colder soil material refers to increased ER, as described by the temperature correction models [19, 31]. But this change of the differential sign in the Bottom Soil layer regarding the ER values indicates that also the temperature difference might be changed in this depth or another factor than temperature like soil moisture has impact on the ER results. It might be that the soil moisture in February is a little higher than that in May. This can be explained ancillary by the antecedent precipitation recorded on the test site. The 7-days antecedent cumulated precipitation before the test in February is 30 mm, while that before the test in May is 16 mm.

But, compared to observed temperature-depth profiles by Bense and Kooi [63] still in June soil temperatures decrease within 3–4 m below temperatures measured in January. In February temperature in this depth will be lower and in May temperature won't have risen as much as

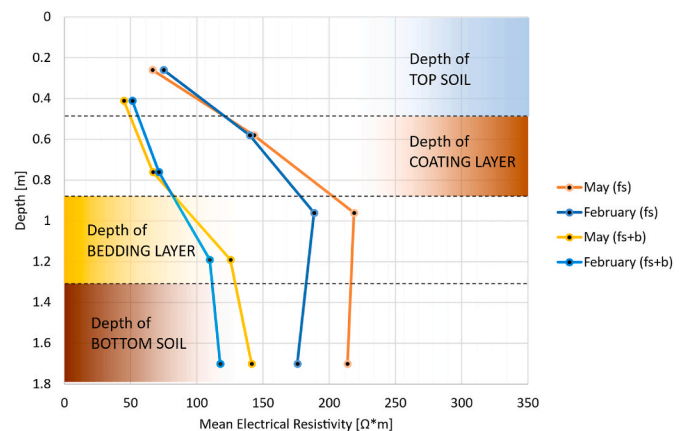


Fig. 13. Mean ER values corrected by temperature. Profiles of Section 1 (above the EAHE installation) for February and May and for each Segment respectively.

in June. Thus, if we assume that temperature is the only influencing factor it is still conceivable, that this intersection of both temperature-depth profiles of February and May is around almost 1.5 m due to the delayed temperature response with depth.

On the other hand, this intersection of the ER differential between the values of February and May in a depth of around 1.4 m could be the indication for another influencing factor like variations in soil moisture. Soil moisture has a variable characteristic through season within the unsaturated soil column which could be detected also by ERT measurements due to its high sensitivity regarding water content. Generally, higher soil water content results in an increased electrical conductivity and with that in a decreased ER [21,25]. It should be assumed that soil moisture in February is higher than in May. If the seasonal impact in ER is driven by soil moisture in February a reduced ER would be expected. But in this case the February ER values are higher within the upper layers. This indicates that at least at depths down to approx. 1.4 m the seasonal changes in ER are driven by temperature and not by soil moisture. However, it is not yet clear whether soil temperature in the direct subsurface of the investigated test area is the only influencing factor or if soil moisture has also its effect. But regarding the conversion of the Bedding Layer, after temperature correction it can be assumed that the soil moisture has an increased influence within the lower layers investigated, especially if the precipitation values from the previous week before the respective measurement are taken into account.

To really prove the impact of soil moisture over season another ERT measurements should have had performed within the late summer, because from winter until June the monitored soil moisture (Fig. 5) is fluctuating around 20 %, which represents the effect of the humid period. The effect of the summer drought does not decrease soil moisture to approx. 10 % until the end of June. Thus, the measurement period could not cover the complete range of soil moisture variation within the installation depth of the test-site.

It is interesting to note that by applying this temperature correction of the ER (Fig. 13) the seasonal differences become minimal within the Coating Layer especially in S1. Thus, as a consequence of a correction by temperature measured at the heat exchanger depth, shifts the intersection depth upwards to exactly the depth where the temperature for correction was measured.

In S2 this intersection depth varies between the Coating Layer and the Bedding Layer. It must be taken into account that the temperature correction was carried out solely on the basis of a single temperature for this depth level of the Coating Layer and not for an entire temperature profile. This also means that the temperature correction for the Coating Layer was calculated with suitable temperatures, but since the same the temperature is used for the other layers, correction probably deviates from the natural circumstances.

The result shows that the temperature correction of ER counteracts the seasonal effect. Even though this is not necessarily surprising, since representative temperatures for the respective month were used for ER correction. In (long-term) ERT studies, it is therefore important to consider the effect of a temperature correction on the scientific question of the study.

As a further result this study shows that seasonal ERT investigations can enable conclusions about the influence of soil temperature within different depth layers through the year, although, it is suggested that measuring of temperature changes by ERT measurements can be challenging [46,64,65]. Arato, Boaga, Comina, De Seta, Di Sipio, Galgaro, Giordano and Mandrone [41] also pointed out this issue especially in unsaturated zones. Usually, temperature effects can be measured by ERT, but particularly when relative temperature differences are large [29]. But in this case a seasonal temperature impact of a difference within installation depth (depth of Coating Layer) of around 5° could have been detected by resistivity measurements.

4.5. EAHE running impact

Regarding the impact of the EAHE system operation itself no significant effect was identified. Still, it seems to be visible within the segment with only fine sand, because there the highest absolute differences occur within the Coating and Bedding Layer in the results of S1. There, the ER values on the first day are consistently lower than on the second day. This is true for May and February as well. Regarding the second segment with fine sand and bentonite as a grouting material nearly no deviations occur. Furthermore, the results between running and not running the system do not differ to a significantly greater extent as the deviations within the reference, which should represent the background noise. Thus, a significant impact of the EAHE impact could not have been achieved after 12 h within this measurement setting.

It has to be considered that in contrast to other studies, the temperature emitted is quite low in this case. This is due to the fact, that this installation consists of only one single pipe and not of a pipe accumulation like within a trench collector. Moreover, for this approach no high air velocity was applied, especially. Thus, also no high temperatures were applied on the system like other approaches did [28,47]. A higher air velocity within the EAHE system might have had a more significant difference as a result.

In this case, the impact of the EAHE installation is mainly present due to the changed soil type in the Coating and Bedding Layer and not due to the operation of the system.

5. Conclusions

The aim of the study to assess relevant soil texture and grouting material characteristics with regard to very shallow geothermal systems by using ERT measurements was successfully reached. By applying ERT a fast area-wide investigation with focus on the relevant influencing parameters for very shallow geothermal potential estimations can be carried out. One advantage of this non-invasive measurement method is that tests can also be carried out after the GSHE has been installed. This also allows the grouting material to be inspected with regard to its thermal properties. Nevertheless, the investigated influence of temperature also shows the challenges of the methodology.

First of all, relative homogeneous natural soil conditions were found within the reference soil section S2, although in installation depth there are mediate ER values due to some more fine-grained layers within the context of a soil profile dominated by gravelly soil.

Regarding the soil section S1 where the GSHE is buried, the influence of the used grouting materials on the ER was ascertained. The ERT measurement shows that the upper three layers (Topsoil, Coating Layer, Bedding Layer) are disturbed by the EAHE installation, whereas the Bottom Soil is in accordance with the natural conditions. Thus, the depth of disturbance was identified. The difference in ER between a grouting material of only fine sand and a second grouting material of the same sand and 10 % bentonite is significant. With regard to the Coating Layers of segment 1 and 2 of S1 this change in grouting material causes a shift of approx. 70 Ω m.

By comparing ER values between the two tests in February and in May, it has been shown that the temperature correction of ER values is necessary to evaluate the impact of temperature and to get a consistent analysis about the soil moisture in the field. The corrected ER result shows that the temperature correction of ER counteracts the seasonal effect, which underlines the sense of the correction. In fact, ER values without temperature correction could also indicate that the soil moisture in February is lower than that in May for all the soil layers. But by applying the temperature correction a similar soil moisture level until Coating Layer between the two tests has been found. Furthermore, ER values with temperature correction show a more humid bottom layer in February, which is supported by the recorded precipitation on the site.

Finally, little impact of the EAHE operating has been detected by ERT measurements. This means that ERT tests could be carried out when the

EAHE system is still running.

This study shows furthermore, that ERT measurements enable an ideal assessment of the essential soil and grouting material characteristics for evaluation of subsurface installations that are depending on heat propagation or thermal properties of soil like very shallow geothermal applications or high voltage underground cable constructions. Especially with regard to soil type, soil moisture and of cause temperature variations, ERT measurements are a valuable tool in this context.

Funding

This study was supported by BayFrance, the university centre for Bavarian-French scientific cooperation (FK19_2018).

CRedit authorship contribution statement

Hans Schwarz: Data curation, Formal analysis, Investigation,

Methodology, Validation, Visualization, Writing – original draft. **Jian Lin:** Conceptualization, Investigation, Methodology, Project administration, Validation, Writing – review & editing. **David Bertermann:** Conceptualization, Funding acquisition, Project administration, Resources, Supervision.

Declaration of competing interest

The authors declare that they have no known competing financial interest or personal relationship that could have appeared to influence the work reported in this paper.

Acknowledgements

We are thankful that we could use the test-site with the EAHE installation of the University of Strasbourg at the ICUBE(UMR7357), IUT Robert Schuman. Further, we thank our colleague Jan Wagner for assistance in the course of our field measurements.

Appendix

Table 3

Comparison of February and May ER values once corrected by temperature and once not, to highlight the seasonal impact in the course of ERT measurement **S1**.

Data status	Layer	ER values of May 2019		ER values of February 2020		Difference (May–February)			
	Segment	Fs [Ω^*m]	Fs + b [Ω^*m]	Fs [Ω^*m]	Fs + b [Ω^*m]	Fs [$\Delta \Omega^*m$]	Fs [%]	Fs + b [$\Delta \Omega^*m$]	Fs + b [%]
NOT corrected by tempera-ture	Topsoil	88.1	59.2	112.7	76.7	-24.6	-27.9	-17.6	-29.7
	Coating Layer	195.3	90.2	219.1	111.0	-23.8	-12.2	-20.7	-23.0
	Bedding Layer	292.2	184.6	306.3	191.5	-14.2	-4.8	-6.9	-3.7
	Bottom Soil	280.7	190.6	266.1	179.2	14.6	5.2	11.4	6.0
corrected by tempera-ture	Topsoil	66.5	45.0	74.9	51.4	-6.5	-9.7	-5.1	-11.3
	Coating Layer	143.1	66.8	140.0	71.3	6.7	4.7	-2.7	-4.0
	Bedding Layer	218.6	125.4	188.5	109.7	35.0	16.0	18.5	14.8
	Bottom Soil	213.7	141.3	175.9	117.6	42.4	19.8	26.8	18.9

Table 4

Comparison of February and May ER values once corrected by temperature and once not, to highlight the seasonal impact in the course of ERT measurement **S2**.

Data status	Layer	ER values of May 2019		ER values of February 2020		Difference (May–February)			
	Segment	Fs [Ω^*m]	Fs + b [Ω^*m]	Fs [Ω^*m]	Fs + b [Ω^*m]	Fs [$\Delta \Omega^*m$]	Fs [%]	Fs + b [$\Delta \Omega^*m$]	Fs + b [%]
NOT corrected by tempera-ture	Topsoil	44.0	41.9	63.2	56.0	-19.1	-43.5	-14.0	-33.5
	Depths of Coating Layer	65.7	72.9	83.2	99.9	-17.4	-26.5	-27.0	-37.0
	Depths of Bedding Layer	140.6	117.3	141.4	134.4	-0.9	-0.6	-17.1	-14.5
	Bottom Soil	304.2	169.1	259.7	142.2	44.4	14.6	26.9	15.9
corrected by tempera-ture	Topsoil	33.5	31.9	42.4	37.5	-8.9	-26.5	-5.6	-17.6
	Depths of Coating Layer	49.7	52.7	55.6	64.5	-5.9	-11.8	-11.9	-22.5
	Depths of Bedding Layer	115.4	76.1	100.8	73.3	14.6	12.7	2.8	3.6
	Bottom Soil	228.7	125.0	172.7	89.8	56.0	24.5	35.2	28.2

References

[1] T. Amanzholov, A. Seitov, A. Aliuly, Y. Yerdesh, M. Murugesan, O. Botella, M. Feidt, H.S. Wang, Y. Belyayev, A. Toleukhanov, Thermal response measurement and performance evaluation of borehole heat exchangers: a case study in Kazakhstan, *Energies* 15 (22) (2022) 8490.

[2] O. Suft, D. Bertermann, One-year monitoring of a ground heat exchanger using the in situ thermal response test: an experimental approach on climatic effects, *Energies* 15 (24) (2022) 9490.

[3] S. Wilke, K. Menberg, H. Steger, P. Blum, Advanced thermal response tests: a review, *Renew. Sustain. Energy Rev.* 119 (2020) 109575.

[4] R. Al-Khoury, N. BniLam, M.M. Arzanfudi, S. Saeid, Analytical model for arbitrarily configured neighboring shallow geothermal installations in the presence of groundwater flow, *Geothermics* 93 (2021) 102063.

- [5] M.L. Fasci, A. Lazzarotto, J. Acuña, J. Claesson, Simulation of thermal influence between independent geothermal boreholes in densely populated areas, *Appl. Therm. Eng.* 196 (2021) 117241.
- [6] H. Schwarz, N. Jovic, D. Bertermann, Development of a calculation concept for mapping specific heat extraction for very shallow geothermal systems, *Sustainability* 14 (7) (2022).
- [7] Y. Zhou, A. Bidarmaghz, N. Makasis, G. Narsilio, Ground-source heat pump systems: the effects of variable trench separations and pipe configurations in horizontal ground heat exchangers, *Energies* 14 (13) (2021) 3919.
- [8] M. Cuny, J. Lin, M. Siroux, V. Magnenet, C. Fond, Influence of coating soil types on the energy of earth-air heat exchanger, *Energy Build.* 158 (2018) 1000–1012.
- [9] M. Cuny, J. Lin, M. Siroux, C. Fond, Influence of an improved surrounding soil on the energy performance and the design length of earth-air heat exchanger, *Appl. Therm. Eng.* 162 (2019) 114320.
- [10] E. Di Sipio, D. Bertermann, Factors influencing the thermal efficiency of horizontal ground heat exchangers, *Energies* 10 (11) (2017) 1897.
- [11] L. Mascarin, E. Garbin, E. Di Sipio, G. Dalla Santa, D. Bertermann, G. Artioli, A. Bernardi, A. Galgaro, Selection of backfill grout for shallow geothermal systems: materials investigation and thermo-physical analysis, *Construct. Build. Mater.* 318 (2022) 125832.
- [12] F. Delalex, X. Py, R. Olives, A. Dominguez, Enhancement of geothermal borehole heat exchangers performances by improvement of bentonite grouts conductivity, *Appl. Therm. Eng.* 33 (2012) 92–99.
- [13] VDI 4640-2, VDI 4640 Part 2 - Thermal Use of the Underground - Ground Source Heat Pump Systems, Beuth Verlag GmbH, Düsseldorf, 2019. V.D.I.e.V.V.-G.E.U.U. (GEU).
- [14] D. Bertermann, H. Klug, L. Morper-Busch, A pan-European planning basis for estimating the very shallow geothermal energy potentials, *Renew. Energy* 75 (2015) 335–347.
- [15] D. Bertermann, H. Klug, L. Morper-Busch, C. Bialas, Modelling vSGPs (very shallow geothermal potentials) in selected CSAs (case study areas), *Energy* 71 (2014) 226–244.
- [16] D. Assouline, N. Mohajeri, A. Gudmundsson, J.-L. Scartezzini, A machine learning approach for mapping the very shallow theoretical geothermal potential, *Geoth. Energy* 7 (1) (2019) 1–50.
- [17] I. Çağlar, M. Demürörer, Geothermal exploration using geoelectric methods in Kestanelbol, Turkey, *Geothermics* 28 (6) (1999) 803–819.
- [18] R.F. Corwin, D.B. Hoover, The self-potential method in geothermal exploration, *Geophysics* 44 (2) (1979) 226–245.
- [19] D.L. Corwin, S.M. Lesch, Apparent soil electrical conductivity measurements in agriculture, *Comput. Electron. Agric.* 46 (1–3) (2005) 11–43.
- [20] S.P. Friedman, Soil properties influencing apparent electrical conductivity: a review, *Comput. Electron. Agric.* 46 (1–3) (2005) 45–70.
- [21] D. Bertermann, H. Schwarz, Bulk density and water content-dependent electrical resistivity analyses of different soil classes on a laboratory scale, *Environ. Earth Sci.* 77 (2018) 1–14.
- [22] M. Chrétien, J. Lataste, R. Fabre, A. Denis, Electrical resistivity tomography to understand clay behavior during seasonal water content variations, *Eng. Geol.* 169 (2014) 112–123.
- [23] G. Dumont, T. Pilawski, T. Hermans, F. Nguyen, S. Garré, The effect of initial water distribution and spatial resolution on the interpretation of ERT monitoring of water infiltration in a landfill cover, *Hydrol. Earth Syst. Sci. Discuss.* (2018) 1–26.
- [24] S. Kraxberger, D. Taferner, H. Klug, 3D electrical resistivity tomography in the monsee catchment, *GI Forum* 2017 (5) (2017) 69–78.
- [25] M. McCutcheon, H. Farahani, J. Stednick, G. Buchleiter, T. Green, Effect of soil water on apparent soil electrical conductivity and texture relationships in a dryland field, *Biosyst. Eng.* 94 (1) (2006) 19–32.
- [26] H. Schwarz, D. Bertermann, Mediate relation between electrical and thermal conductivity of soil, *Geomechanics and Geophysics for Geo-Energy and Geo-Resources* 6 (2020) 1–16.
- [27] K. Hayley, L.R. Bentley, M. Gharibi, M. Nightingale, Low temperature dependence of electrical resistivity: implications for near surface geophysical monitoring, *Geophys. Res. Lett.* 34 (18) (2007).
- [28] T. Hermans, A. Vandenbohede, L. Lebbe, F. Nguyen, A shallow geothermal experiment in a sandy aquifer monitored using electric resistivity tomography, *Geophysics* 77 (1) (2012) B11–B21.
- [29] M. Nouveau, G. Grandjean, P. Leroy, M. Philippe, E. Hedri, H. Boukicm, Electrical and thermal behavior of unsaturated soils: experimental results, *J. Appl. Geophys.* 128 (2016) 115–122.
- [30] N. Giordano, C. Comina, G. Mandrone, Laboratory scale geophysical measurements aimed at monitoring the thermal affected zone in Underground Thermal Energy Storage (UTES) applications, *Geothermics* 61 (2016) 121–134.
- [31] K.R. Sheets, J.M. Hendrickx, Noninvasive soil water content measurement using electromagnetic induction, *Water Resour. Res.* 31 (10) (1995) 2401–2409.
- [32] N.H. Abu-Hamdeh, R.C. Reeder, Soil thermal conductivity effects of density, moisture, salt concentration, and organic matter, *Soil Sci. Soc. Am. J.* 64 (4) (2000) 1285–1290.
- [33] D. Barry-Macaulay, A. Bouazza, R.M. Singh, B. Wang, P. Ranjith, Thermal conductivity of soils and rocks from the Melbourne (Australia) region, *Eng. Geol.* 164 (2013) 131–138.
- [34] D. Bertermann, H. Schwarz, Laboratory device to analyse the impact of soil properties on electrical and thermal conductivity, *Int. Agrophys.* 31 (2) (2017).
- [35] J. Côté, J.-M. Konrad, Thermal conductivity of base-course materials, *Can. Geotech. J.* 42 (1) (2005) 61–78.
- [36] S.D. Logsdon, T.R. Green, J.V. Bonta, M.S. Seyfried, S.R. Evett, Comparison of electrical and thermal conductivities for soils from five states, *Soil Sci.* 175 (12) (2010) 573–578.
- [37] D.N. Singh, S.J. Kuriyan, K.C. Manthena, A generalised relationship between soil electrical and thermal resistivities, *Exp. Therm. Fluid Sci.* 25 (3–4) (2001) 175–181.
- [38] S. Sreedeeep, A. Reshma, D. Singh, Generalized relationship for determining soil electrical resistivity from its thermal resistivity, *Exp. Therm. Fluid Sci.* 29 (2) (2005) 217–226.
- [39] Q. Sun, C. Lü, Semiempirical correlation between thermal conductivity and electrical resistivity for silt and silty clay soils, *Geophysics* 84 (3) (2019) MR99–MR105.
- [40] T. Tokoro, T. Ishikawa, S. Shirai, T. Nakamura, Estimation methods for thermal conductivity of sandy soil with electrical characteristics, *Soils Found.* 56 (5) (2016) 927–936.
- [41] A. Arato, J. Boaga, C. Comina, M. De Seta, E. Di Sipio, A. Galgaro, N. Giordano, G. Mandrone, Geophysical monitoring for shallow geothermal applications—Two Italian case histories, *First Break* 33 (8) (2015) 75–79.
- [42] C. Comina, N. Giordano, G. Ghidone, F. Fischanger, Time-lapse 3d electric tomography for short-time monitoring of an experimental heat storage system, *Geosciences* 9 (4) (2019) 167.
- [43] M. Cultrera, J. Boaga, E. Di Sipio, G. Dalla Santa, M. De Seta, A. Galgaro, Modelling an induced thermal plume with data from electrical resistivity tomography and distributed temperature sensing: a case study in northeast Italy, *Hydrogeol. J.* 26 (3) (2018) 837–851.
- [44] C. Sáez Blázquez, I. Martín Nieto, A. Farfán Martín, D. González-Aguilera, P. Carrasco García, Comparative analysis of different methodologies used to estimate the ground thermal conductivity in low enthalpy geothermal systems, *Energies* 12 (9) (2019) 1672.
- [45] N. Giordano, A. Arato, C. Comina, G. Mandrone, Time-lapse electrical resistivity imaging of the thermally affected zone of a Borehole Thermal Energy Storage system near Torino (Northern Italy), *J. Appl. Geophys.* 140 (2017) 123–134.
- [46] T. Hermans, F. Nguyen, T. Robert, A. Revil, Geophysical methods for monitoring temperature changes in shallow low enthalpy geothermal systems, *Energies* 7 (7) (2014) 5083–5118.
- [47] H. Schwarz, B. Badenes, J. Wagner, J.M. Cuevas, J. Urchueguía, D. Bertermann, A case study of thermal evolution in the vicinity of geothermal probes following a distributed TRT method, *Energies* 14 (9) (2021) 2632.
- [48] M. Benhammou, B. Draoui, Parametric study on thermal performance of earth-to-air heat exchanger used for cooling of buildings, *Renew. Sustain. Energy Rev.* 44 (2015) 348–355.
- [49] T.S. Bisioniya, A. Kumar, P. Baredar, Experimental and analytical studies of earth-air heat exchanger (EAHE) systems in India: a review, *Renew. Sustain. Energy Rev.* 19 (2013) 238–246.
- [50] A. Mostafaeipour, H. Goudarzi, M. Khanmohammadi, M. Jahangiri, A. Sedaghat, H. Norouzzianpour, S. Chowdhury, K. Techat, A. Issakhov, K. Almutairi, Techno-economic analysis and energy performance of a geothermal earth-to-air heat exchanger (EAHE) system in residential buildings: a case study, *Energy Sci. Eng.* 9 (10) (2021) 1807–1825.
- [51] C. Peretti, A. Zarrella, M. De Carli, R. Zecchin, The design and environmental evaluation of earth-to-air heat exchangers (EAHE). A literature review, *Renew. Sustain. Energy Rev.* 28 (2013) 107–116.
- [52] W. Zeitoun, J. Lin, M. Siroux, Energetic and exergetic analyses of an experimental earth-air heat exchanger in the northeast of France, *Energies* 16 (3) (2023) 1542.
- [53] W. Zeitoun, J. Lin, M. Siroux, A review—earth-air heat exchanger: applications, advances and challenges, in: *IOP Conference Series: Earth and Environmental Science*, IOP Publishing, 2022 012005.
- [54] VDI 4640-4, VDI 4640 Part 4 - thermal use of the underground - direct uses, in: *V. Verein Deutscher Ingenieure_ (Ed.), VDI-Gesellschaft Energie und Umwelt*, 2004, p. 40.
- [55] J. Lin, H. Nowamooz, S. Braymand, P. Wolff, C. Fond, Impact of soil moisture on the long-term energy performance of an earth-air heat exchanger system, *Renew. Energy* 147 (2020) 2676–2687.
- [56] M. Cuny, J. Lin, M. Siroux, C. Fond, Influence of rainfall events on the energy performance of an earth-air heat exchanger embedded in a multilayered soil, *Renew. Energy* 147 (2020) 2664–2675.
- [57] T. Dahlin, M.H. Loke, Resolution of 2D Wenner resistivity imaging as assessed by numerical modelling, *J. Appl. Geophys.* 38 (4) (1998) 237–249.
- [58] T. Dahlin, B. Zhou, A numerical comparison of 2D resistivity imaging with 10 electrode arrays, *Geophys. Prospect.* 52 (5) (2004) 379–398.
- [59] M.H. Loke, Tutorial: 2-D and 3-D Electrical Imaging Surveys, 2004.
- [60] GGU, *Die Widerstandsgeoelektrik*, 2011. https://www.ggu.karlsruhe.de/GGU_Die_Widerstandsgeoelektrik_WID98-C.pdf. (Accessed 16 February 2023), 2023.
- [61] C.-H.M. Tso, O. Kuras, P.B. Wilkinson, S. Uhlemann, J.E. Chambers, P.I. Meldrum, J. Graham, E.F. Sherlock, A. Binley, Improved characterisation and modelling of

- measurement errors in electrical resistivity tomography (ERT) surveys, *J. Appl. Geophys.* 146 (2017) 103–119.
- [62] K.E. Saxton, W.J. Rawls, Soil water characteristic estimates by texture and organic matter for hydrologic solutions, *Soil Sci. Soc. Am. J.* 70 (5) (2006) 1569–1578.
- [63] V. Bense, H. Kooi, Temporal and spatial variations of shallow subsurface temperature as a record of lateral variations in groundwater flow, *J. Geophys. Res. Solid Earth* 109 (B4) (2004).
- [64] T. Hermans, S. Wildemeersch, P. Jamin, P. Orban, S. Brouyère, A. Dassargues, F. Nguyen, Quantitative temperature monitoring of a heat tracing experiment using cross-borehole ERT, *Geothermics* 53 (2015) 14–26.
- [65] T. Robert, C. Paulus, P.-Y. Bolly, E. Koo Seen Lin, T. Hermans, Heat as a proxy to image dynamic processes with 4D electrical resistivity tomography, *Geosciences* 9 (10) (2019) 414.